Supporting Information

Enhanced molecular doping for high conductivity in polymers with volume freed for dopants

Hui Li,[†, ‡] Mallory E. DeCoster,[§] Chen Ming,[†] Mengdi Wang,[†] Yanling Chen,[†] Patrick E. Hopkins,[§] Lidong Chen[, †, ⊥] and Howard E. Katz[*, ‡]*

[†]State Key Laboratory of High Performance Ceramics and Superfine Microstructures, Shanghai Institute of Ceramics, Chinese Academy of Sciences, Shanghai 200050, China

[‡]Department of Materials Science and Engineering, Johns Hopkins University, 3400 North Charles Street, Baltimore, Maryland 21218, United States

[§]Department of Mechanical and Aerospace Engineering, University of Virginia, Charlottesville, Virginia 22904, United States

[⊥]Center of Materials Science and Optoeletronics Engineering, University of Chinese Academy of Sciences, Beijing 100049, China

Experimental details

Materials and Methods: Unless stated otherwise, starting materials and solvents were obtained from Adamas, Aldrich and Acros and were used without any further purification. The monomer 2,5-dibromothieno[3,2-b]thiophene and bithiophene were purchased from Suna Tech Inc. 5,5'-Bis(trimethylstannyl)-2,2'-bithiophene and 2,5-bis(trimethylstannyl)-thieno[3,2-b]thiophene were synthesized according to the literatures.[1] Thiophene substituted by alkyl group or alkylthiol group was prepared according to the published procedures.[2] ^{1}H NMR (400 MHz) spectra of monomers were recorded on a Bruker Avance spectrometer using $CDCl_3$ as solvent and tetramethylsilane (TMS) as the internal standard. UV-vis-NIR absorption spectra were taken on Agilent Cary 5000 spectrophotometer. The absorption intensity was normalized by the film thickness. Cyclic voltammetry (CV) was performed in a one-chamber, three-electrode cell in dry acetonitrile containing 0.1 M *n*-Bu_4NPF_6 as a supporting electrolyte. A glass carbon disk, a platinum wire and Ag/AgCl electrode, were used as the working electrode, auxiliary electrode and reference electrode, respectively. A ferrocene/ferrocenium redox couple as an external standard, whose oxidation potential is set at -4.8 eV with respect to zero vacuum level. The calculation of HOMO energy levels of polymers follows the literature.[3] The thickness of films was measured by Bruker DektakXT stylus profiler. Grazing-Incidence Wide-Angle X-ray Scattering (GIWAXS) data were recorded at beamline BL14B1 of the Shanghai Synchrotron Radiation Facility (SSRF) at a wavelength of 1.24 Å. The out-of-plane profiles were measured by XRD (Bruker D8 ADVANCE) at a wavelength of 1.54 Å and the in-plane profiles were extracted from the 2D-GIWXRS pattern. All films were heated at 60 ℃ in the glovebox to remove the residue solvent before the GIWAXS measurements.

Device Fabrication and Characterization: The OFET devices were fabricated and tested as the same as before.[4] The mobility was calculated in the saturation regime according to the equation: $I_{DS} = (W/2L)\mu C_i(V_G - V_T)^2$, where I_{DS} is the drain current, μ is the mobility, and V_G and V_T are the gate voltage and threshold voltage, respectively.

For thermoelectric devices, glass substrates (L = 18mm and W = 9 mm) were cleaned by sonication in deionized water, acetone and *i*-propanol. Polymer was dissolved in chlorobenzene with the concentration of 5 mg mL^{-1}. F4TCNQ was dissolved in chlorobenzene with the concentration of 2 mg mL^{-1}. NOBF4 was dissolved in THF with the concentration of 5 mg mL^{-1}. The polymer and F4TCNQ solution were separately heated and sonicated at 70 ºC for 30 min. Then the polymer and dopant were mixed together with the desired concentration. The mixture was sonicated for 20 min. The final solution was dropped on the glass substrate. After evaporation of solvent, the devices were annealed on a hot plate at 60 ºC for 30 min in glovebox to remove the residue solvent. Resistance and Seebeck coefficient were measured by using a four-probe measurement method with using the ZEM-5 TF Seebeck Coefficient/Electrical Resistance Measurement System (Advance Riko). Samples were held at designated temperatures for a total of 1.5 hours for conductivity and Seebeck coefficient stability measurements.

Synthesis of monomers and polymers

Synthesis of **Monomer 1**:

TH-C16-Br (1.0 g, 2.6 mmol) and 5,5'-bis(trimethylstannyl)-2,2'-bithiophene (0.58 g, 1.2 mmol) were added into tube and flushed with N_2, $Pd_2(dba)_3$ (32.0 mg, 0.035 mmol) and P(*o*-tol)$_3$ (42.7 mg, 0.14 mmol) were added. Then degassed toluene (30 mL) was added. The mixture was thoroughly degassed under N_2. The tube was subjected to oil bath heating at 110 ℃ for 48 h. The resulting mixture was cold to room temperature and toluene was removed under reduced pressure, and then the solid was purified by column chromatography (hexane) to afford yellow solid (87%). The product (0.8 g, 1.0 mmol) was dissolved in $CHCl_3$: AcOH (5:1, 30 mL) at 0 °C and NBS (0.4 g, 2.3 mmol) was added in portions under dark. The reaction mixture was stirred for 6 h. After the reaction was finished, the reaction mixture was poured into water and extracted with $CHCl_3$. The organic layers were concentrated under reduced pressure to yield the crude product. The solid was purified by column chromatography (hexane:CH_2Cl_2 = 1:1) to afford **monomer 1** as a yellow solid (0.9g, 89%). ^{1}H NMR (400 MHz, $CDCl_3$, ppm): δ

7.11-7.10 (d, 2H), 6.97-6.96 (d, 2H), 2.73-2.69 (m, 4H), 1.30-1.25 (m, 56H), 0.90-0.86 (m, 6H), 0.90-0.86 (m, trace hexane).

Synthesis of **Monomer 2**:

TH-SC16-Br (1.0 g, 2.4 mmol) and 5,5'-bis(trimethylstannyl)-2,2'-bithiophene (0.5 g, 1.1 mmol) were used as starting materials and then brominated with NBS (0.3g, 1.6 mmol) to obtain **monomer 2** as a light green solid (0.6 g, 86%).^{1}H NMR (400 MHz, $CDCl_3$, ppm): δ 7.22-7.21 (d, 2H), 7.15-7.14 (d, 2H), 2.88-2.85 (m, 4H), 1.31-1.25 (m, 56H), 0.92-0.89 (m, 6H), 0.92-0.89 (m, trace hexane).

Synthesis of **PQTC16-TT**:

To an oven-dried tube was added the following reagents sequentially: monomer 1 (200 mg, 0.21 mmol), 2,5-bis(trimethylstannyl)-thieno[3,2-b]thiophene (99 g, 0.21 mmol), $Pd_2(dba)_3$ (5.9 mg, 0.006 mmol) and P(*o*-tol)$_3$ (7.8 mg, 0.024 mmol). The tube was sealed and flushed with N_2. Then degassed chlorobenzene (8 mL) was added. The mixture was thoroughly degassed under N_2. The tube was subjected to oil bath at 120 °C for 48 h. After cooling to RT, the polymer was precipitated into methanol (100 mL) and filtered. The polymer was purified using Soxhlet extraction with methanol, acetone, hexane, and chloroform. The chloroform solution was concentrated and precipitated into methanol again. The precipitates were filtered and dried under vacuum to afford PQTC16-TT as a dark brown solid (150 mg, 60%).

Synthesis of **PQTSC16-TT**:

The synthesis of **PQTSC16-TT** was similar as **PQTC16-TT.** The resulting polymer was dark brown solid (85 mg, 67%).

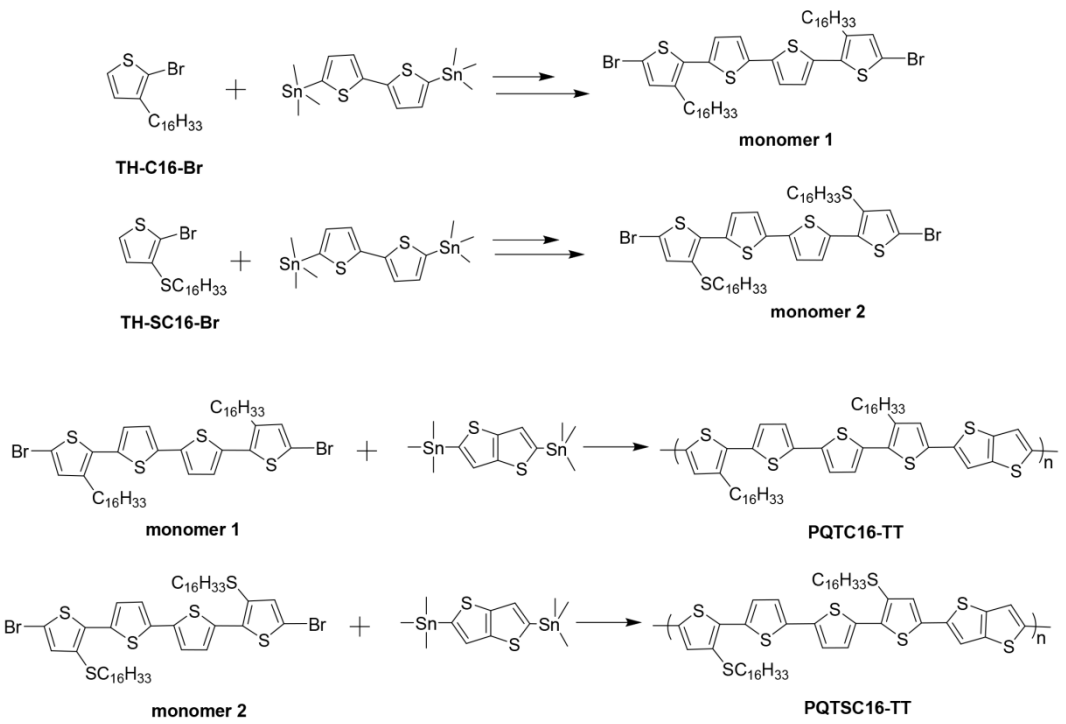

Figure S1. The synthetic routes of **PQTC16-TT** and **PQTSC16-TT**.

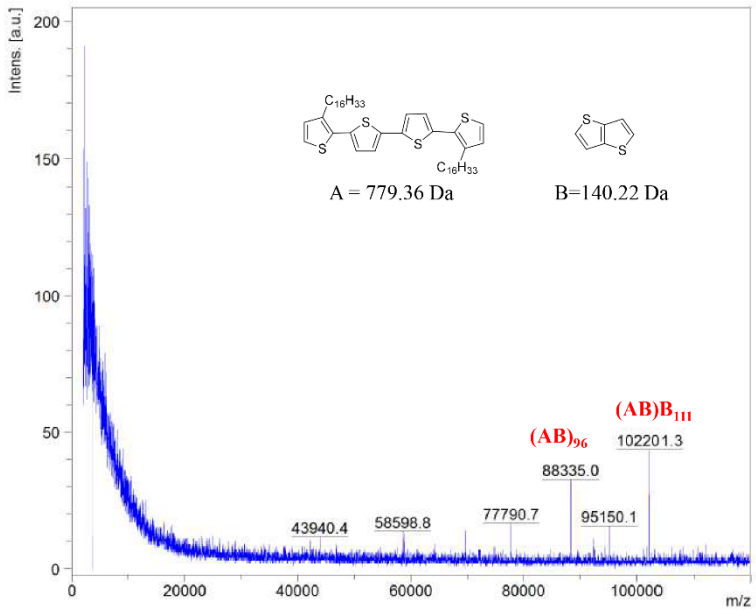

Figure S2. MALDI-TOF result of PQTC16-TT.

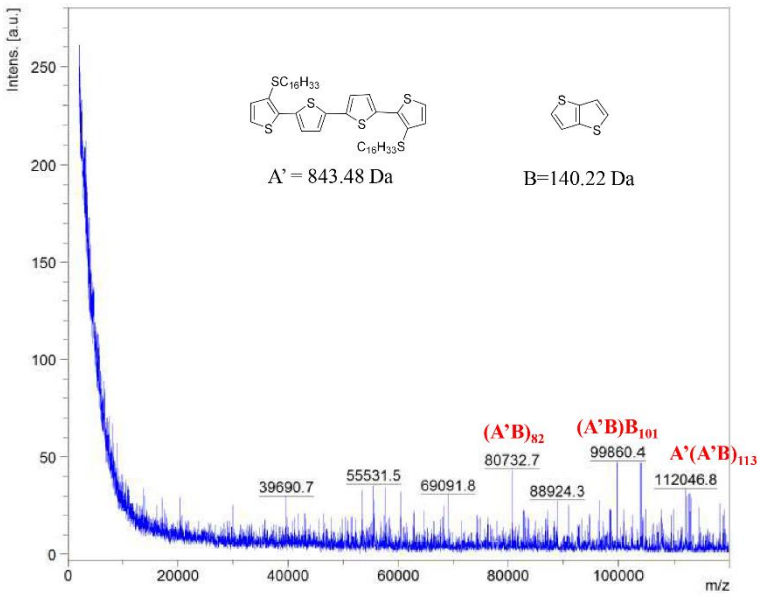

Figure S3. MALDI-TOF result of PQTSC16-TT.

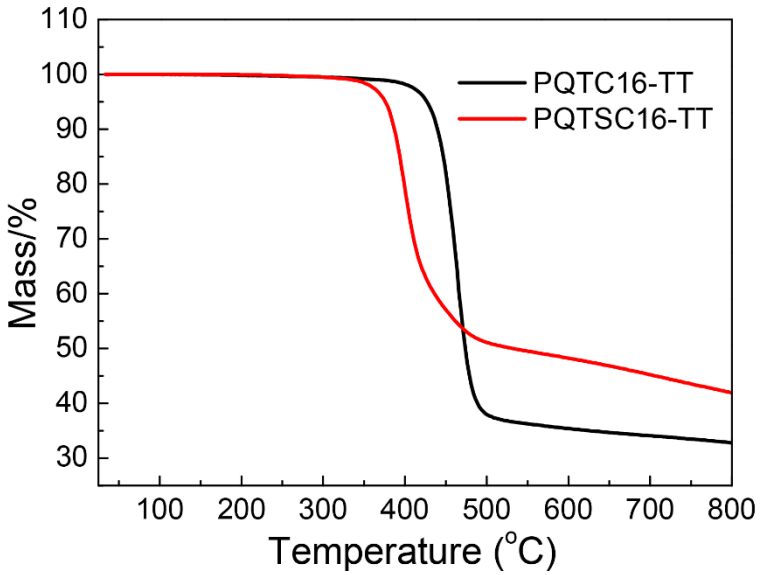

Figure S4. Thermogravimetric analysis (TGA) curves for PQTC16-TT and PQTSC16-TT. Scan rate is 10 ℃/min from room temperature to 800 ℃ in N_2.

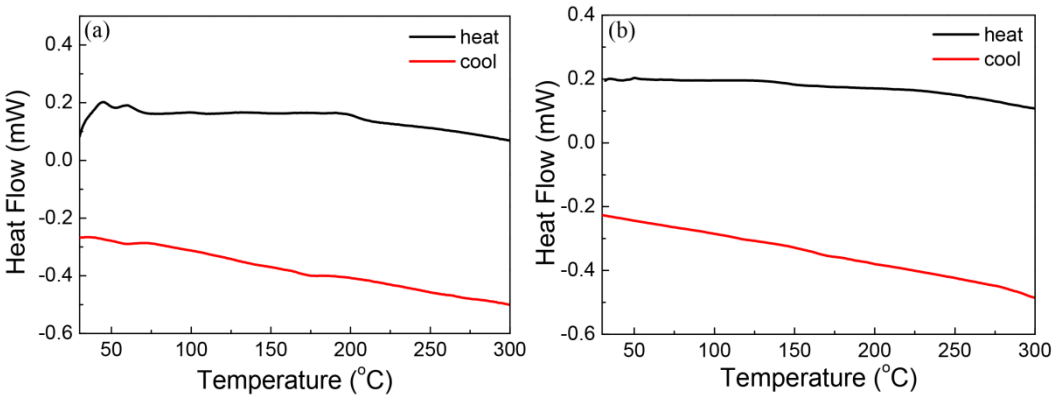

Figure S5. DSC heating and cooling traces of **PQTC16-TT** (a) and **PQTSC16-TT** (b) at a scanning speed of 10 °C/min under N_2.

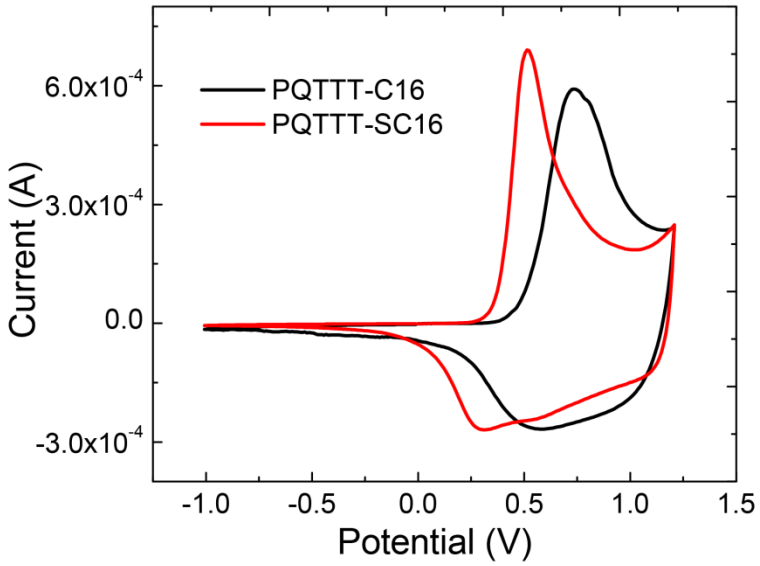

Figure S6. Cyclic voltammetry of **PQTC16-TT** and **PQTSC16-TT**. Polymer thin film was coated onto working electrode and put into acetonitrile with 0.1 M tetrabutylammonium hexafluorophosphate as the supporting electrolyte.

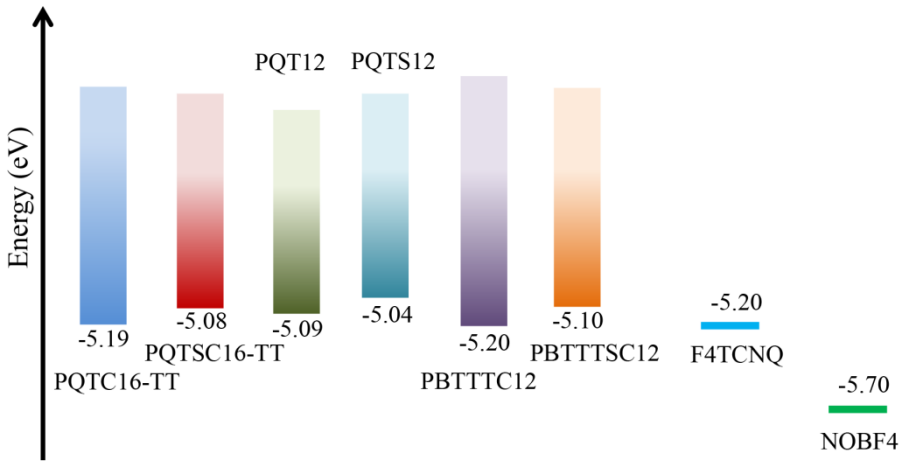

Figure S7 The energy levels of polymers and dopants used in this paper.

Calculation of energy levels

The LUMO level of F4TCNQ is 5.2 eV obtained from the literature.[5] The LUMO level of NOBF4 was calculated according to the redox potential of nitrosonium (NO+) which is 1.27~1.25 V vs SCE (saturated calomel electrode). Based on -4.4 ~ -4.7 eV SCE energy level relative to vacuum, LUMO = - e(E_{red} + 4.5) (eV). The LUMO level of 5.7 eV for NOBF4 can be obtained.[2]

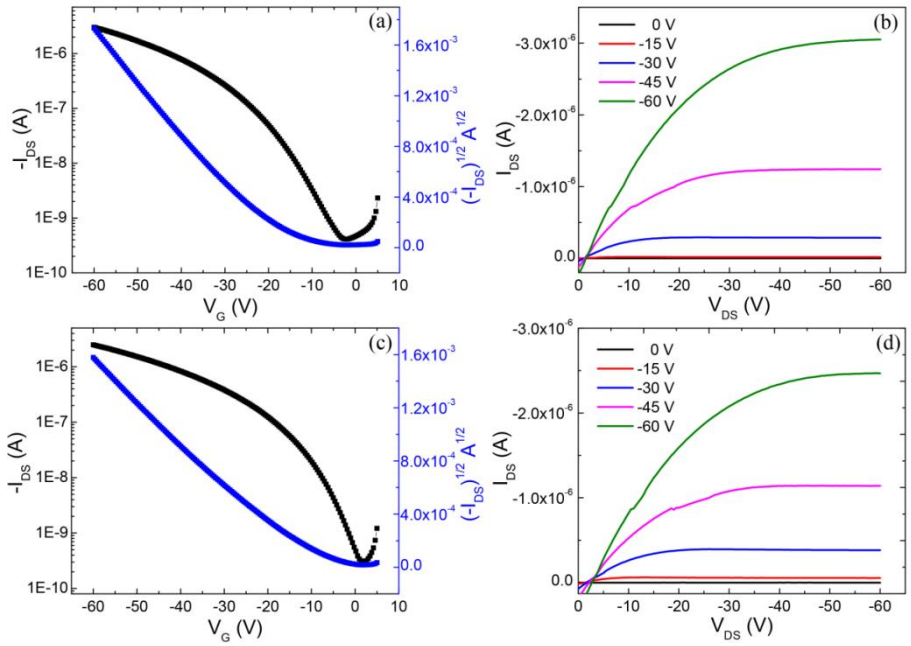

Figure S8. The transfer and output curves of transistors based on **PQTC16-TT** (a, b) and **PQTSC16-TT** (c, d). The drain voltage is -60 V for the transfer curves.

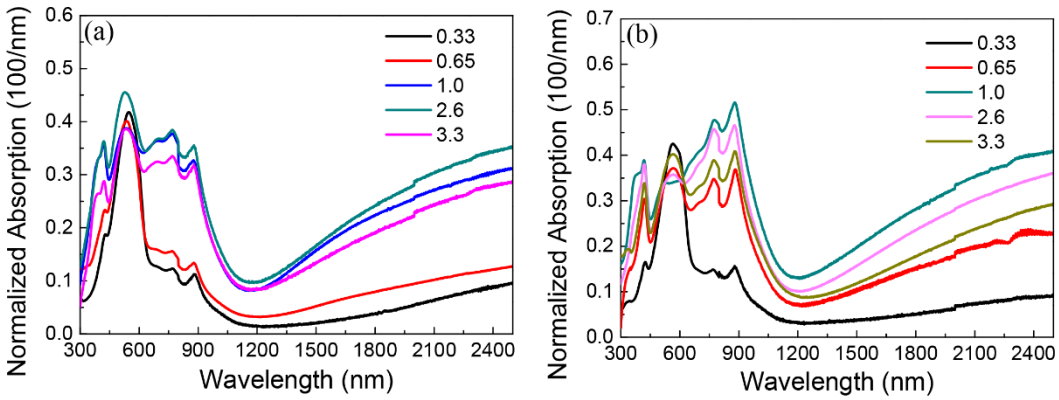

Figure S9. Thickness-normalized absorption of undoped and F4TCNQ-doped polymers. (a) PQTC16-TT/F4TCNQ; (b) PQTSC16-TT/F4TCNQ. The molar ratio is dopant to polymer repeat unit.

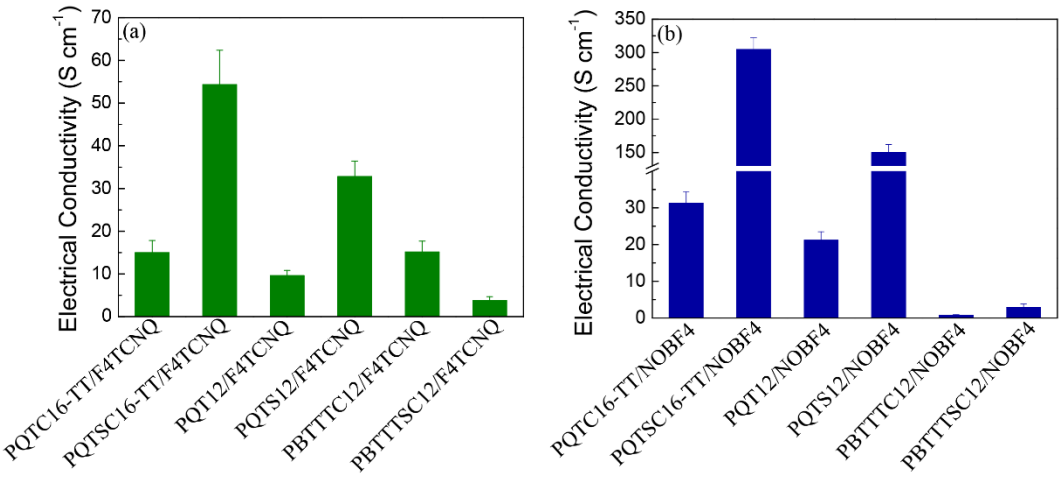

Figure S10. Electrical conductivities of polymers doped with F4TCNQ (a) and NOBF4 (b), respectively. (molar ratio is 1)

Thermal conductivity measurements for doped polymers:

The thermal conductivities of the doped spacer polymers were measured using time domain Thermoreflectance (TDTR), and optical pump-probe thermometry technique. The polymers were spin coated onto the metal side of an Au/SiO_2 substrate. The substrate consisted of 80 nm of Au, which had been electron beam evaporated onto bulk amorphous SiO_2 at a chamber pressure of 6.3e-6 Torr. The 80 nm of Au serves as a transducer during the TDTR measurement, converting the optical energy from the laser

pulse into thermal energy. The temporal decay of this thermal energy is measured to obtain the thermal properties of interest. A detailed schematic of the TDTR experiment is shown in Figure S11. The detailed specifics of this technique are published elsewhere.[6] Briefly, TDTR is a non-contact optical thermometry technique that uses the output of a sub-picosecond laser system in a pump-probe configuration. We used a Ti:Sapphire Spectra Physics Tsunami oscillator that emits laser pulses at a repetition rate of 80 MHz and a wavelength of ~800 nm (FWHM ~10.5 nm). The output from the oscillator is split into two paths (pump and probe), with the pump and probe spot sizes focused down to $1/e^2$ radii of 9.0 μm and 4.3 μm, respectively. The pump path is electro-optically modulated at a frequency of 8.8 MHz with a square wave. The pump then passes through the transparent SiO_2 substrate, creating a modulated heating event at the Au surface, where the heat then transfers to both the SiO_2 and the polymer. The reflectivity of the Au changes linearly with the surface temperature, and is monitored temporally by the probe pulse. The probe is delayed in time up to 6 ns by a translational mechanical delay stage, and the change in absorption of the probe on the Au surface at 8.8 MHz is related to the time-varying temperature changes created by the pump pulses. This temporal change in probe absorption is monitored via the reflected probe intensity off the Au surface and collected with a Thorlabs Det10A photodiode. A lock-in amplifier demodulates the signal from this photodiode, and provides amplitude and phase information in the form of a thermal decay curve. These data are then fit with a multilayer, cylindrically symmetric heat conduction model to obtain the thermal properties of the material.[6-8] In this sample configuration, bidirectional heat conduction must be accounted for in the analysis, since the heat flows into the SiO_2 and the polymer.[9] The results for the thermal conductivities of the doped polymers are provided in Figure S12. The TDTR measurements for this sample system are sensitive to the thermal effusivity of both the SiO_2 and polymer films. This means that the TDTR signal is equally sensitive to the volumetric heat capacity and thermal conductivity of the polymers; therefore to measure one parameter, the other must be known. We assume literature values of the heat capacities of the Au and SiO_2, along with literature values

for the thermal conductivities of the evaporated Au thin films.[7] We characterized the Au/SiO_2 substrates before the polymers were deposited by measuring the thermal conductivity of the SiO_2 and the thermal boundary conductance (TBC) between the Au/SiO_2. The polymers doped at a molar ratio of 1:1 were deposited on substrates where κ_{SiO_2}= 1.40 +/- 0.06 W m^{-1} K^{-1} and TBC = 46.2 +/- 1.72 MW m^{-2} K^{-1}. The polymers that were doped at a molar ratio of 1:3 were deposited on substrates with κ= 1.42 +/- 0.07 $Wm^{-1}K^{-1}$ and TBC = 83.0 +/- 12.4 MW m^{-2} K^{-1}. This is an important distinction because our thermal model is very sensitive to the thermal boundary conductance between the Au and SiO_2 interface. Since the heat capacities of the PQTC16-TT and PQTSC16-TT polymer films are not available in the literature, we assume a heat capacity for that of P3HT, since the chemical structure of their backbone is similar, and propagate 10% uncertainty about this assumed heat capacity into our error analysis.[9] It should be noted that uncertainties in the assumed heat capacity propagate to uncertainties in the measured thermal conductivities. Therefore, the total uncertainty encompassed by our error bars for the reported thermal conductivity measurements contain a +/- 3nm uncertainty in the transducer film thickness, the error in the heat capacity of the polymer, and spot to spot variability on the sample surface. We see an increase in the thermal conductivity as the polymers are doped at higher molar ratios. Sample data measured from the polymers along with their fits are shown in Figure S13.

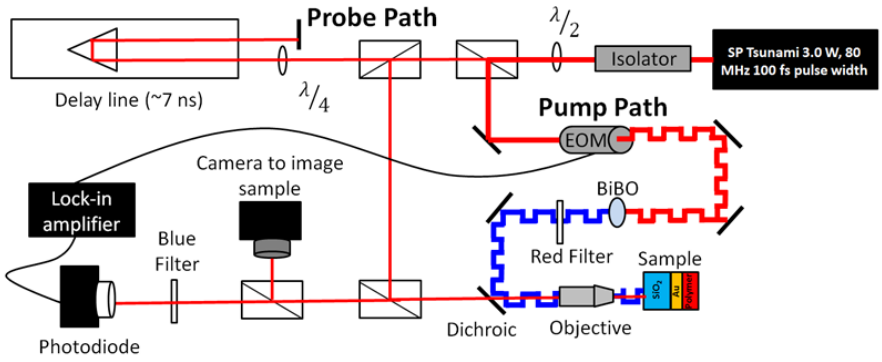

Figure S11. Schematic of the TDTR setup at the University of Virginia.

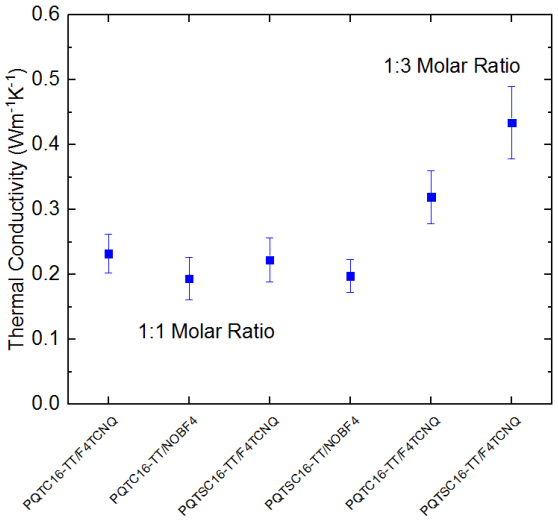

Figure S12. Thermal conductivity results for the doped polymers (molar ratio of 1:3 is repeat unit to dopant molecule).

Table S1. The thermal conductivity data of doped polymers with different molar ratio.

doped film	molar ratio (dopant to repeat unit)	thermal conductivity (W m^{-1} K^{-1})	RMS (W m^{-1} K^{-1})
PQTC16-TT/F4TCNQ	1:1	0.2323	0.0301
PQTSC16-TT/F4TCNQ	1:1	0.2223	0.0343
PQTC16-TT/NOBF4	1:1	0.1934	0.0329
PQTSC16-TT/NOBF4	1:1	0.1978	0.0255
PQTC16-TT/F4TCNQ	3:1	0.4045	0.0487
PQTSC16-TT/F4TCNQ	3:1	0.5297	0.0645

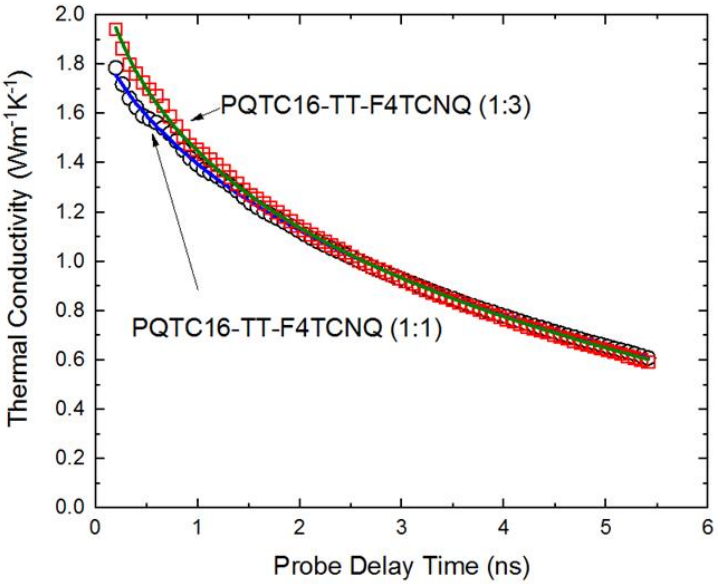

Figure S13. Raw TDTR data shown as open symbols for PQTC16-TT/F4TCNQ with two different molar ratios of dopant (molar ratio is repeat unit to dopant molecule). The thermal models that are fit to the data are shown as solid lines.

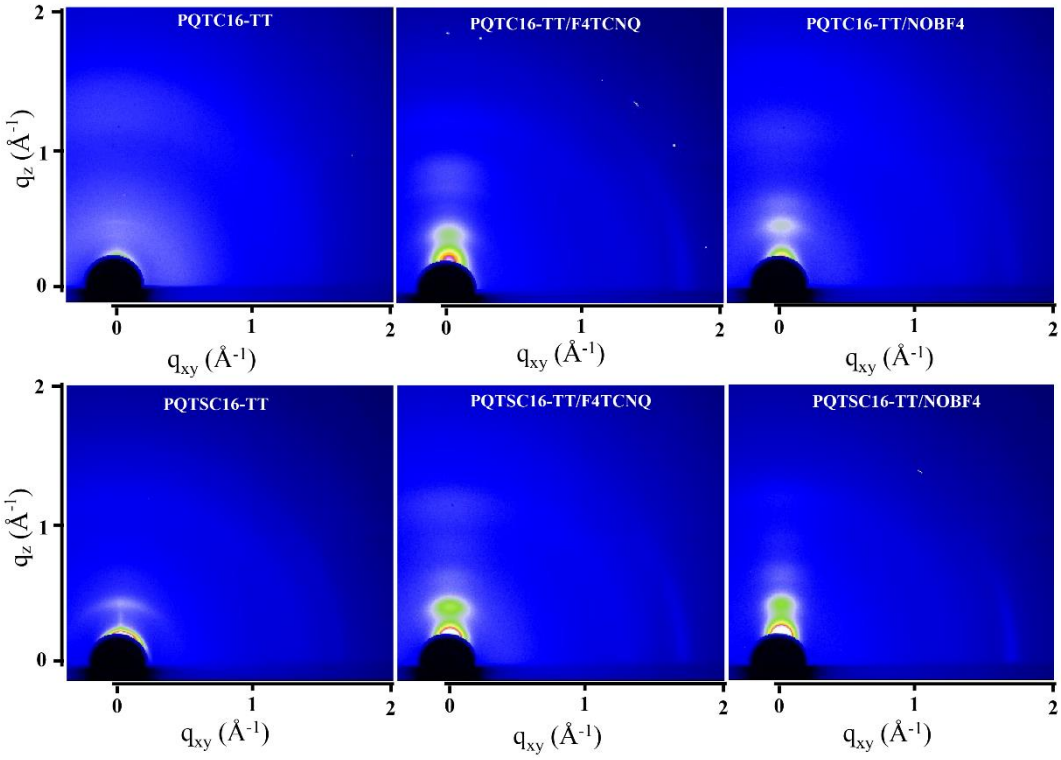

Figure S14. 2D-GIWAXS images of pure polymers and doped polymers. The molar ratio of dopant to repeat unit is 1 to 1.

Table S2. Crystallographic parameters calculated from GIWAXS profiles. (the value in round brackets represents the increase compared with pure polymer)

samples	out of plane		in plane	
	2θ (degree)	lamellar distance (Å)	2θ (degree)	π-π stacking (Å)
PQTC16-TT	3.69	23.92	–	–
PQTSC16-TT	3.59	24.58	19.75	3.62
PQTC16-TT/F4TCNQ	3.36	26.29 (2.37)	20.72	3.45
PQTSC16-TT/F4TCNQ	3.48	25.35 (0.77)	20.79	3.44
PQTC16-TT/NOBF4	3.32	26.59 (2.67)	20.85	3.43
PQTSC16-TT/NOBF4	3.57	24.70 (0.12)	21.02	3.40

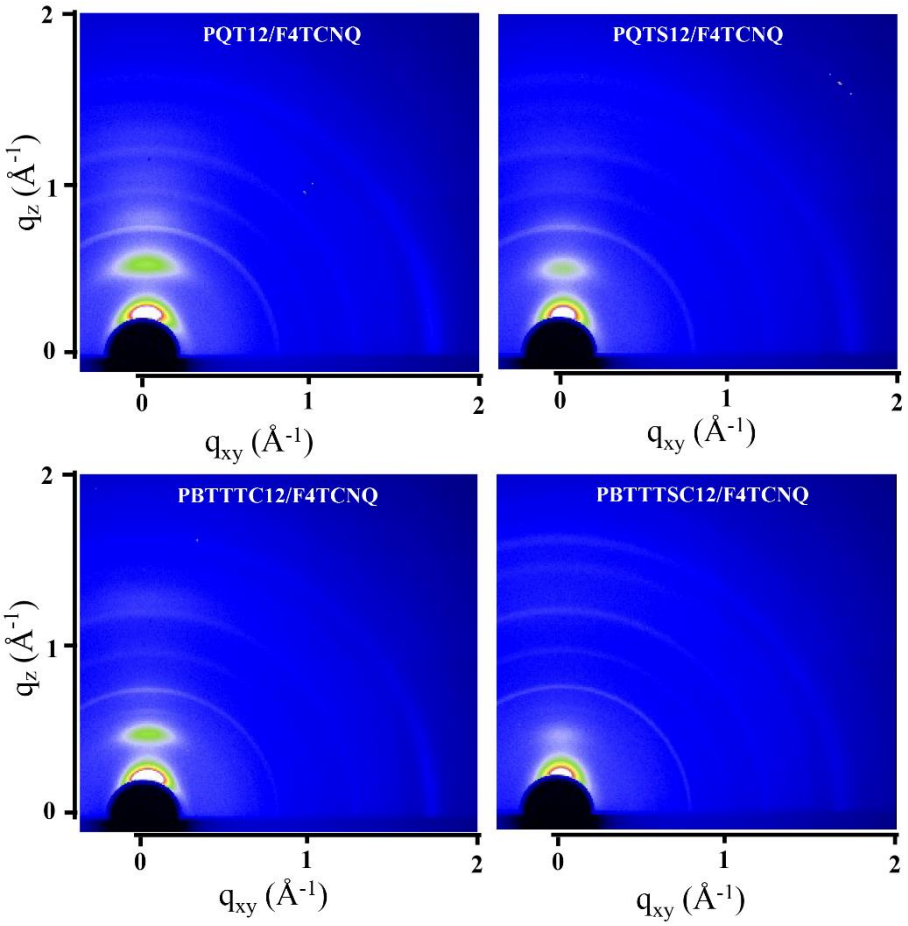

Figure S15. 2D-GIWAXS images of PQT12/F4TCNQ, PQTS12/F4TCNQ, PBTTTC12/F4TCNQ and PBTTTSC12/F4TCNQ. The molar ratio of dopant to repeat unit is 1 to 1.

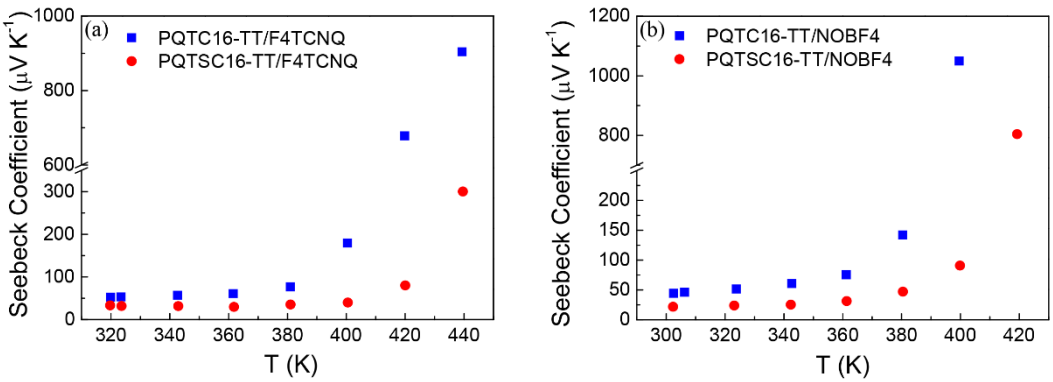

Figure S16. Temperature-dependent Seebeck coefficient of **PQTC16-TT** and **PQTSC16-TT** doped with F4TCNQ (a) and NOBF4 (b), respectively.

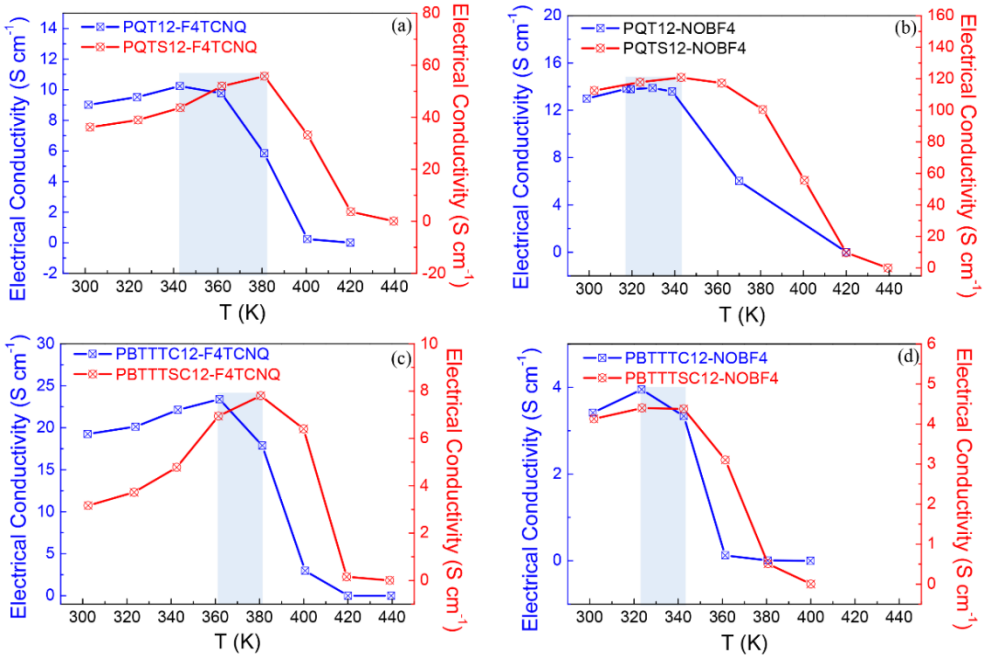

Figure S17. Temperature-dependent electrical conductivity of PQT(S)12 (a, b) and PBTTT(S)C12 (c, d) doped with F4TCNQ and NOBF4. The shaded region indicates increased stability of doped PQTSC16-TT formulations.

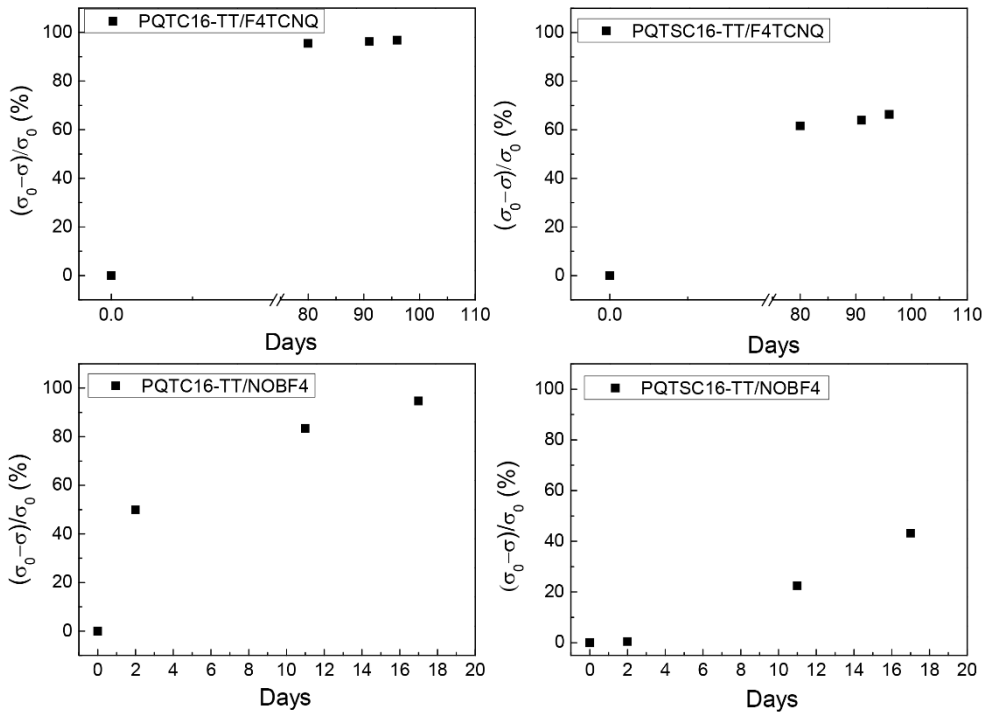

Figure S18. Environmental stability of doped films stored in air with ~60% humidity (σ_0: original conductivity, σ: real-time conductivity).

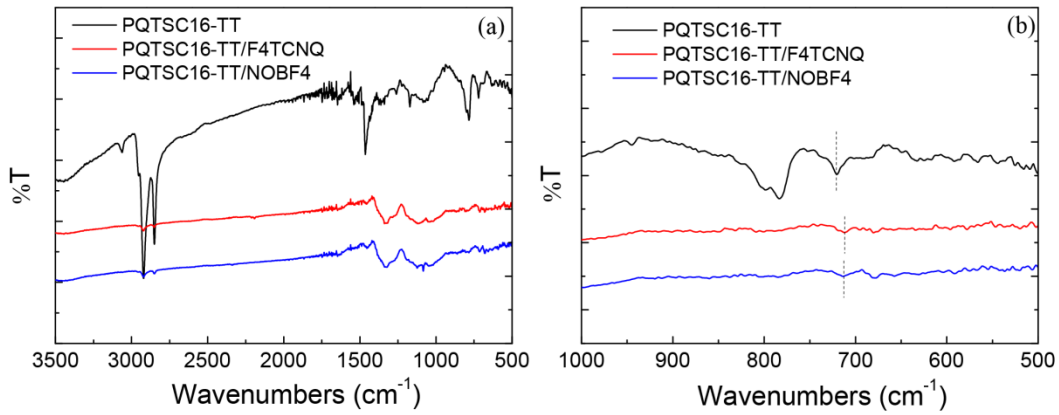

Figure S19. (a) Fourier transform infrared spectroscopy (FTIR) of pure PQTSC16-TT and doped PQTSC16-TT. (b) The FTIR spectra ranging from 1000 ~ 500 cm^{-1}.

Calculation of different geometries:

The adsorption structures and energy of molecules (F4TCNQ and NOBF4) on polymer chains were optimized and calculated by density functional theory (DFT) using the Vienna ab initio Simulation Package (VASP). One dopant adsorbed on one repeat unit

of the polymer was used as the calculation model employing a periodical boundary condition. That is, the calculation focused on an isolated polymer chain with periodic dopants interacting with repeat units instead of the slab calculations of a sheet of polymer molecules. A plane-wave basis and projector augmented wave method (PAW) pseudopotentials were used. The Perdew-Burke-Ernzerhof (PBE) generalized gradient approximation (GGA) was adopted to treat exchange-correlation effects and DFT-D2 method was used to describe van der Waals interactions. A cutoff of 350 eV was imposed on the kinetic energy. Sampling of the Brillouin zone (BZ) was performed using 4 × 1 × 1 Monkhorst-Pack grids. The structures were optimized by a conjugate-gradient (CG) algorithm with an imposed numerical threshold of 0.01 eV/Å.

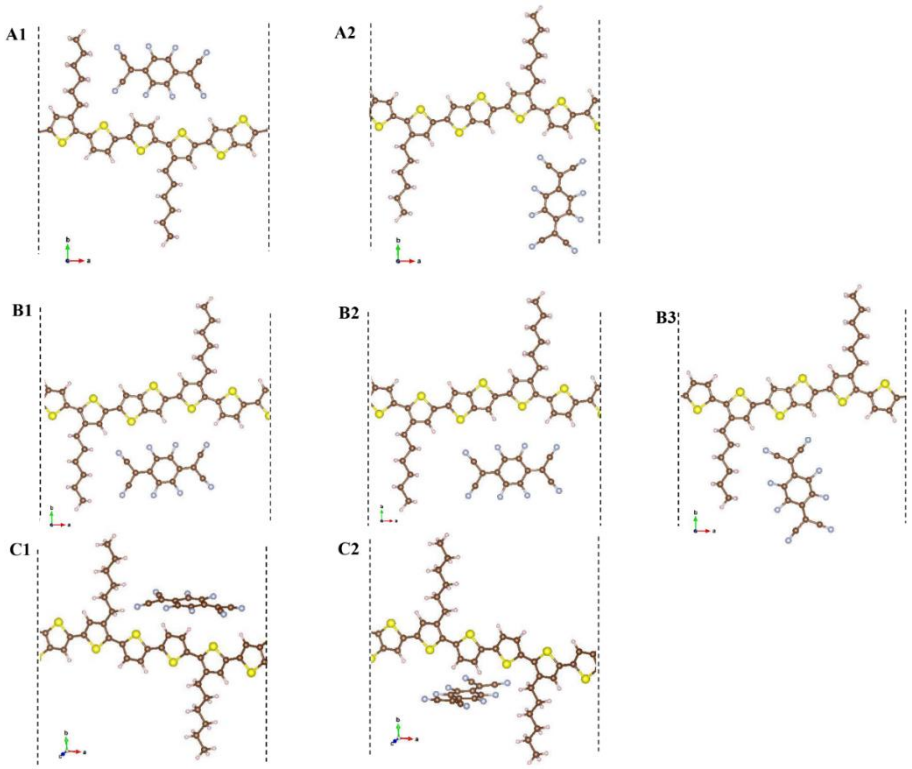

Figure S20. Image cuts of the optimized molecular geometries of F4TCNQ-doped **PQTC16-TT** with molar ratio of 1 when F4TCNQ was placed at different positions. The hexyl chains were used for the sake of clarity.

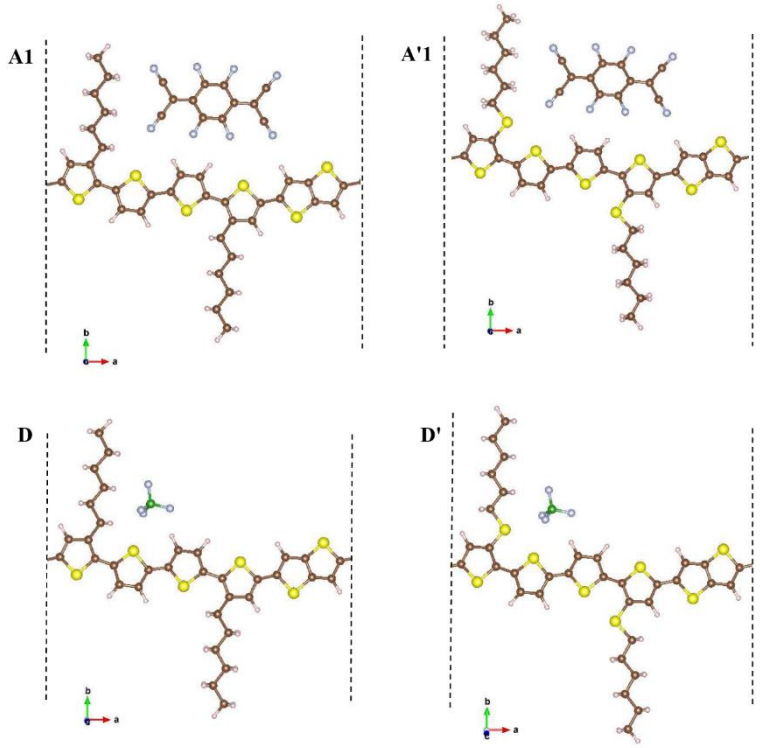

Figure S21. Optimized geometries of F4TCNQ-doped **PQTC16-TT** (A1), F4TCNQ-doped **PQTSC16-TT** (A'1), NOBF4-doped **PQTC16-TT** (D) and NOBF4-doped **PQTSC16-TT** (D') with molar ratio of 1. The hexyl chains were used for the sake of clarity.

Table S3. Optimized energy of geometries shown in Figure S15 and Figure S16. ΔE means the energy difference between the complex and the original energy of dopant and polymer chain ($\Delta E = E_{\text{dopant}} + E_{\text{polymer chain}} - E_{\text{complex}}$).

geometries	ΔE (eV)	charge transfer (e)
A1	1.60	0.69
A2	1.37	–
B1	1.59	0.68
B2	1.24	–
B3	1.38	–
C1	1.40	–
C2	1.04	–
A'1	1.64	0.75
D	4.09	0.96
D'	4.06	0.96

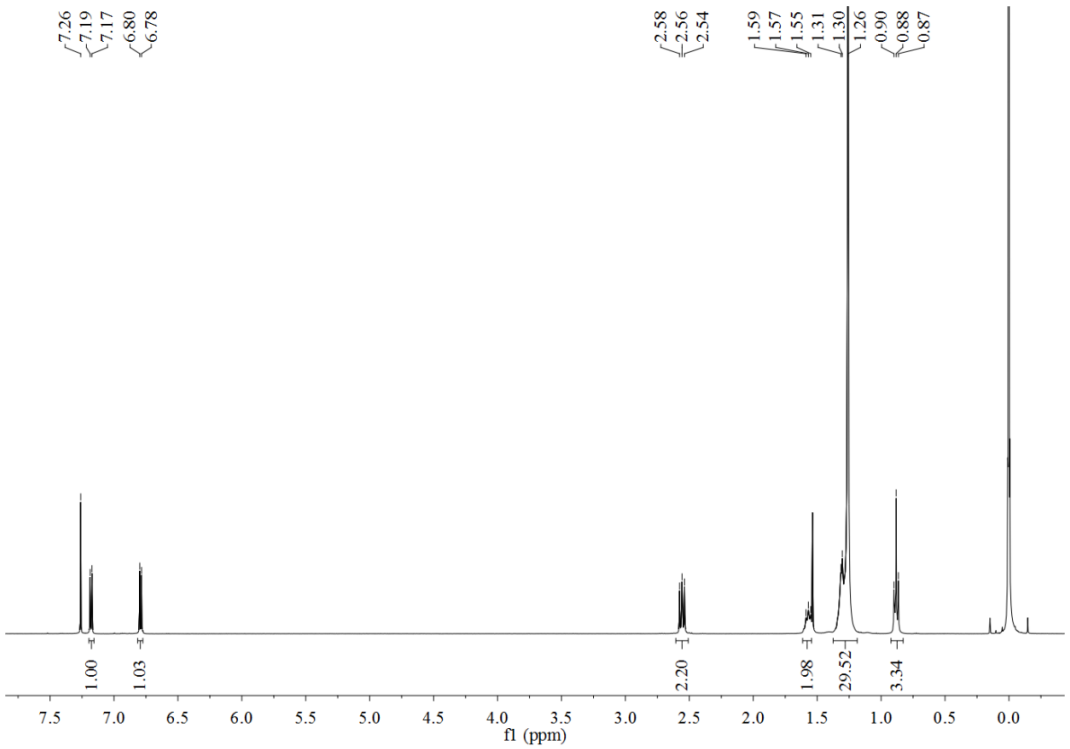

Figure S22. ^{1}H NMR of TH-C16-Br

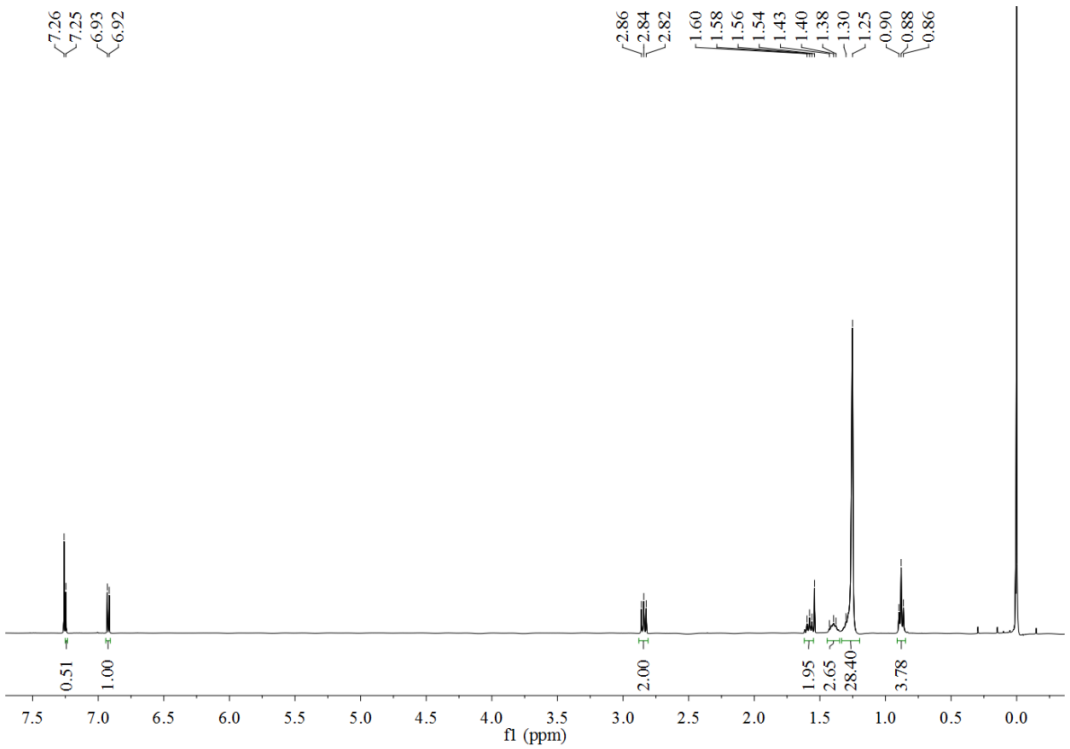

Figure S23. ^{1}H NMR of TH-SC16-Br

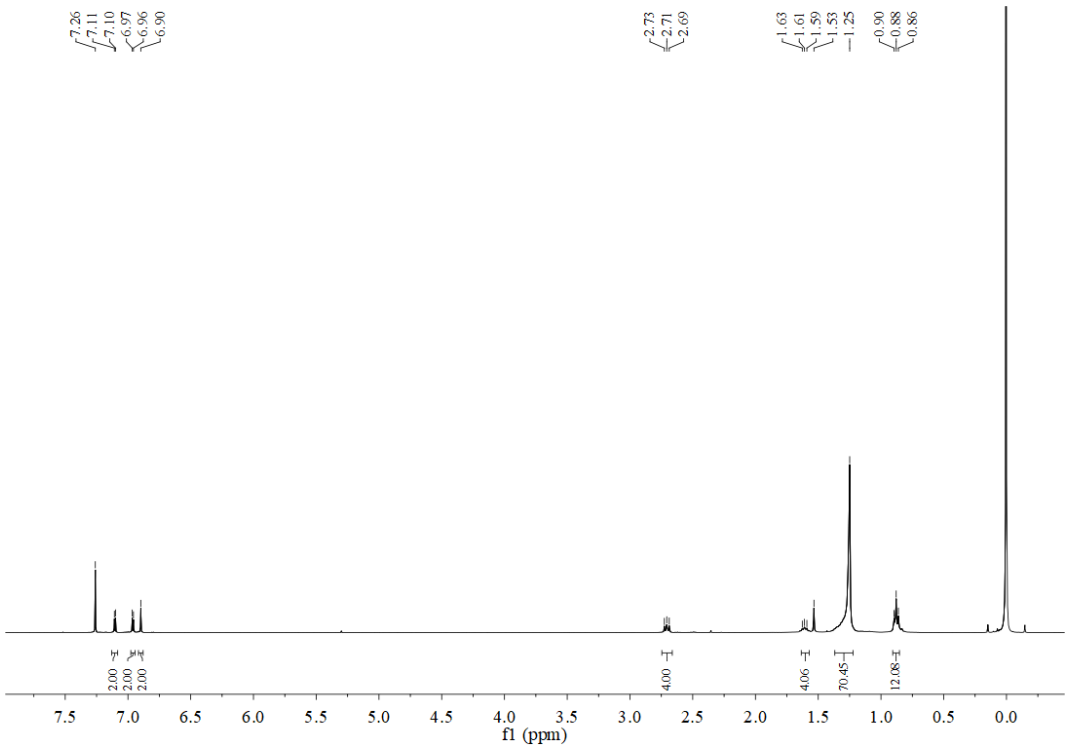

Figure S24. ^{1}H NMR of monomer 1. (the solvent peak of hexane overlaps with the protons of side chains of monomer 1)

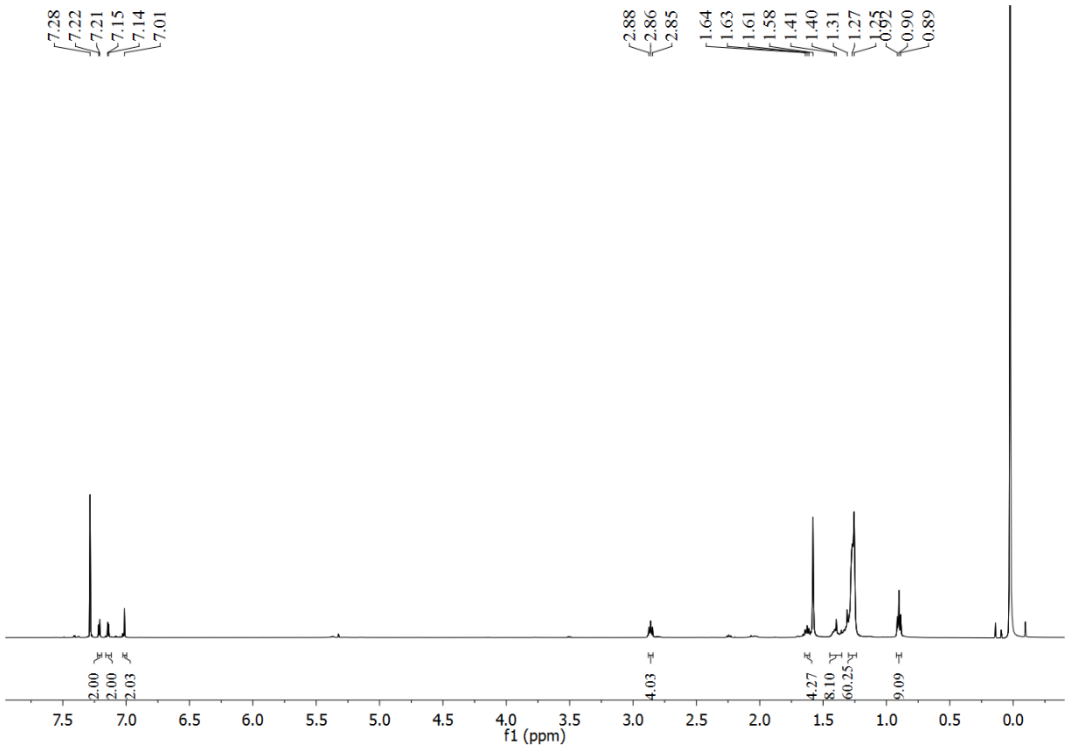

Figure S25. ^{1}H NMR of monomer 2. (the peak of trace hexane overlaps with the protons of side chains of monomer 2)

References:

(1) Fei, Z.; Pattanasattayavong, P.; Han, Y.; Schroeder, B. C.; Yan, F.; Kline, R. J.; Anthopoulos, T. D.; Heeney, M. Influence of Side-Chain Regiochemistry on the Transistor Performance of High-Mobility, All-Donor Polymers. *J. Am. Chem. Soc.* **2014,** *136*, 15154-15157.

(2) Li, H.; DeCoster, M. E.; Ireland, R. M.; Song, J.; Hopkins, P. E.; Katz, H. E. Modification of the Poly(bisdodecylquaterthiophene) Structure for High and Predominantly Nonionic Conductivity with Matched Dopants. *J. Am. Chem. Soc.* **2017**, *139*, 11149-11157.

(3) Dou, L.; You, J.; Yang, J.; Chen, C.-C.; He, Y.; Murase, S.; Moriarty, T.; Emery, K.; Li, G.; Yang, Y. Tandem polymer solar cells featuring a spectrally matched low-bandgap polymer. *Nat. Photon.* **2012,** *6*, 180-185.

(4) Li, H.; Plunkett, E.; Cai, Z.; Qiu, B.; Wei, T.; Chen, H.; Thon, S. M.; Reich, D. H.; Chen, L.; Katz, H. E. Dopant-Dependent Increase in Seebeck Coefficient and Electrical Conductivity in Blended Polymers with Offset Carrier Energies. *Adv. Electronic Mater*. **2019**, 1800618.

(5) Li, J.; Rochester, C. W.; Jacobs, I. E.; Aasen, E. W.; Friedrich, S.; Stroeve, P.; Moulé, A. J. The effect of thermal annealing on dopant site choice in conjugated polymers. *Org. Electron.* **2016,** *33*, 23-31.

(6) Schmidt, A.; Chiesa, M.; Chen, X.; Chen, G. An optical pump-probe technique for measuring the thermal conductivity of liquids. *Rev. Sci. Instrum.* **2008,** *79*, 064902.

(7) Cahill, D. G. Analysis of heat flow in layered structures for time-domain thermoreflectance. *Rev. Sci. Instrum.* **2004**, *75*, 5119-5122.

(8) Hopkins, P. E.; Serrano, J. R.; Phinney, L. M.; Kearney, S. P.; Grasser, T. W.; Harris, C. T. Criteria for Cross-Plane Dominated Thermal Transport in Multilayer Thin Film Systems During Modulated Laser Heating. *J. Heat Transf.* **2010,** *132*, 081302-081310.

(9) Hopkins, P. E.; Kaehr, B.; Phinney, L. M.; Koehler, T. P.; Grillet, A. M.; Dunphy, D.; Garcia, F.; Brinker, C. J. Measuring the Thermal Conductivity of Porous, Transparent SiO2 Films With Time Domain Thermoreflectance. *J. Heat Transf.* **2011,** *133*, 061601-061608.